

Flexible machine learning estimation of conditional average treatment effects: a blessing and a curse

R.A.J. Post^{1, 2}, I.L. van den Heuvel¹, M. Petkovic¹, and E.R. van den Heuvel^{1, 3}

¹*Department of Mathematics and Computer Science, Eindhoven University of Technology, The Netherlands*

²*Institute for Complex Molecular Systems, Eindhoven University of Technology, The Netherlands*

³*Department of Preventive Medicine and Epidemiology, School of Medicine, Boston University, USA*

Abstract

Causal inference from observational data requires untestable assumptions. If these assumptions apply, machine learning (ML) methods can be used to study complex forms of causal-effect heterogeneity. Several ML methods were developed recently to estimate the conditional average treatment effect (CATE). If the features at hand cannot explain all heterogeneity, the individual treatment effects (ITEs) can seriously deviate from the CATE. In this work, we demonstrate how the distributions of the ITE and the estimated CATE can differ when a causal random forest (CRF) is applied. We extend the CRF to estimate the difference in conditional variance between treated and controls. If the ITE distribution equals the CATE distribution, this difference in variance should be small. If they differ, an additional causal assumption is necessary to quantify the heterogeneity not captured by the CATE distribution. The conditional variance of the ITE can be identified when the individual effect is independent of the outcome under no treatment given the measured features. Then, in the cases where the ITE and CATE distributions differ, the extended CRF can appropriately estimate the characteristics of the ITE distribution while the CRF fails to do so.

Keywords— Causal inference, Machine learning, Heterogeneity of treatment effects, Unmeasured effect modifiers, Individual treatment effect

1 Introduction

The increasing availability of (big) observational data has tremendously boosted the field of machine learning (ML) (Mooney and Pejaver, 2018). ML provides us with flexible, non-parametric methods to study the observed outcome Y , given features, \mathbf{X} , that may involve a treatment (or exposure), A , by statistical inference on the (conditional) distributions of $Y \mid \mathbf{X}, A = a$. Therefore, ML methods are excellent at predicting future observations that arise from the same (factual) distribution (Dickerman and Hernán, 2020). However, it is essential to realize that these models cannot be automatically used to answer ‘what if’ questions for the treatment A , i.e. for counterfactual prediction, as associations found in the data are not necessarily causal (Hernán et al., 2019; Dickerman and Hernán, 2020; Prospero et al., 2020; Cui and Athey, 2022; van Geloven et al., 2020; Mooney et al., 2021; Dickerman et al., 2022). Statistical inference of associations is thus only one step in causal inference and, as such, in counterfactual prediction (Balzer and Petersen, 2021).

The critical step for causal inference is linking the distribution of outcomes in a universe where everyone was treated with a , i.e. potential outcomes (Hernán and Robins, 2020), $Y^a \mid \mathbf{X}$ to the distribution of the observed data. To do so, when working with observational data, we have to make untestable assumptions so that the data and, thus, ML cannot help us out. Instead, we have to rely on the knowledge of experts (Hernán and Robins, 2020). Suppose these assumptions can be made, and the distributions of potential and observed outcomes can be linked. In that case, causal estimands (targets) of interest can be connected to

estimands of the data-generating distribution and estimated with statistical inference. Next to the validity of the causal assumptions, accurate statistical inference is thus necessary for causal inference. When the assumptions are applicable, but the statistical inference is off, e.g., when using misspecified models for the observed outcomes, the causal inference will also be invalid. The flexibility offered by ML methods can thus improve causal inference by correctly estimating conditional means of our observations (Mooney et al., 2021; Blakely et al., 2019). More precisely, ML methods can be exploited to flexibly learn nuisance parameters of the data generating distribution, such as conditional means and propensity scores, which in turn can be used to estimate the causal estimand, as is, for example, done in targeted maximum likelihood estimation (TMLE) (van der Laan and Rose, 2011; Schuler and Rose, 2017).

The increasing availability of diverse data makes studying effect heterogeneity among individuals more feasible. The precision medicine field aims to understand this heterogeneity to improve individual treatment decisions (Kosorok and Laber, 2019). The average treatment effect (ATE), $\mathbb{E}[Y^1 - Y^0]$ might seriously differ from the individual treatment effect (ITE), $Y^1 - Y^0$ (Kravitz et al., 2004). Therefore, the focus has shifted to the estimation of the conditional average treatment effect (CATE), $\mathbb{E}[Y^1 - Y^0 \mid \mathbf{X}]$, given features \mathbf{X} of an individual (Robertson et al., 2020). The functional form of effect modification by different levels of these features might be very complex, so ML methods are promising tools for estimating CATEs (Bica et al., 2021).

In recent years several meta-learning strategies for CATE estimation have been proposed. These strategies decompose the CATE estimation into regression problems that can be solved with any suitable machine learning method (see Caron et al. (2022) for a detailed review). T-learners fit separate models for treated and controls and estimate CATEs as the plug-in difference of the conditional mean estimates, see, e.g. Athey and Imbens (2016) and Powers et al. (2018). The performance of T-learners will depend on the levels of sparsity and smoothness of conditional means for treated and controls, as well as the choice of the base learner. T-learners generally fail for subgroups where the treated and control samples differ in size, as illustrated by Künzel et al. (2019). X-learners have been proposed to deal with the difference in sample size by first using a T-learner to predict individual treatment effects that are subsequently used to derive the CATEs for treated and controls separately from which a weighted average is derived (Künzel et al., 2019). S-learners include treatment assignment as another covariate next to other features and the CATE is estimated as the difference of the estimated conditional means for treated and controls, see e.g. Hill (2011), Foster et al. (2011), Green and Kern (2012) and Imai and Ratkovic (2013). Estimation with S-learners might suffer from serious finite-sample bias because they do not involve the CATE directly but focus on the conditional means, a problem also known for ATE estimation (Chernozhukov et al., 2018). To remedy this issue, Hahn et al. (2020) introduced the Bayesian causal forest model that extends the work of Hill (2011) by including the CATE as an explicit parameter on the model with its own prior. The R-learner directly identifies the CATE by regressing transformed outcomes on transformed treatment assignment using estimates of nuisance parameters in a first step (as we will elaborate on in Section 2) (Nie and Wager, 2020). The R-learner is also called ‘double machine learning’ and may give unbiased estimates of the average causal effect for finite samples. At the same time, a one-step approach (S-learner) would still be biased (Chernozhukov et al., 2018). Similarly, the DR-learner deals with augmented inverse probability weighted transformation (Robins et al., 1994) of observations after constructing estimates of the propensity score and conditional means in a first step (Kennedy, 2020; Fan et al., 2022). The cost of making weaker assumptions using the flexible ML methods is slower convergence rates for the estimators, known as the curse of dimensionality (Naimi et al., 2021). Therefore, much of the ongoing research is focused on comparing the different methods for CATE estimation to derive whether and when they are optimal, see e.g. Wendling et al. (2018), Knaus et al. (2020), Kennedy (2020), and Curth and van der Schaar (2021).

The aim of this work is entirely different, as we want to emphasize the difference between the CATE and the ITE. The CATE is much more personalized than the ATE and, thus, an important step towards precision medicine. However, it concerns us that the notion of CATE is sometimes perceived as equivalent to the ITE, see, e.g. Lu et al. (2018). Whether the CATE is an appropriate proxy for the ITE depends on

the remaining variability of causal effects given the considered modifiers, e.g. a CATE ≥ 0 given $\mathbf{X} = \mathbf{x}$ (Talisa and Chang, 2021) does not imply that all ITEs ≥ 0 for those individuals (Hand, 1992). In this work, we investigate whether we can use a causal random forest (CRF) (Athey et al., 2019) to estimate characteristics of the marginal ITE distribution. More specifically, we investigate the performance of the CRF to estimate $\text{var}(Y^1 - Y^0)$ and $\mathbb{P}(Y^1 - Y^0 > 0)$ that could be essential population characteristics next to the ATE and CATE. To do so, we have simulated data from a known causal system based on estimates from a real case study and fit the CRF to estimate individual CATEs and compared the distributions of the (random) conditional expectation, $\mathbb{E}[Y^1 - Y^0 \mid \mathbf{X}]$, and the ITE, $Y^1 - Y^0$.

It is well known that an ITE is not identifiable because of the fundamental problem of causal inference (Holland, 1986). However, it is good to realize this is also the case for the ATE and CATE in the presence of unmeasured confounding that we can never rule out when working with observational data. The ATE and CATE become identifiable once the unconfoundedness assumption is supported by expert knowledge. To open up the field of ITE and CATE deviation, we show that under a conditional independent effect deviation assumption (ITE independent of Y^0 given the CATE), the (conditional) variance of the ITE becomes identifiable. To give an idea of how this could evolve the field of treatment effect heterogeneity, we extend the CRF algorithm to estimate an individual Gaussian distribution (centred at the CATE) that will be degenerate in the absence of remaining effect heterogeneity.

In Section 2, we introduce our notion and present the necessary causal inference assumptions for CATE estimation. Furthermore, we describe the methodology behind the CRF algorithm and our reality-based data simulation. Section 3 presents the results of fitting the CRF to datasets simulated under different settings. In Section 4, we introduce a new causal assumption such that the conditional variance of the ITE becomes identifiable and extend the CRF to estimate individual conditional distributions of the ITE. Furthermore, we present the results of analyzing the simulated datasets with this new algorithm. Finally, we present some concluding remarks and ideas for future research in Section 5.

2 Notation and Methods

Probability distributions of factual and counterfactual outcomes are defined in the potential outcome framework (Neyman, 1923; Rubin, 1974). Let Y_i and A_i represent the (factual) stochastic outcome and the random treatment assignment level of individual i . Let Y_i^a equal the potential outcome under an intervention on the treatment to level a (Y_i^a is counterfactual when $A_i \neq a$). We will consider only two treatment levels $\{0, 1\}$ with 0 indicating no treatment. Thus, the individual causal effect of an arbitrary individual i is defined as $Y_i^1 - Y_i^0$ (Hernán and Robins, 2020). We must make some assumptions to relate the distribution of potential outcomes to the distribution of observed outcomes. First of all, it is necessary to have access to a set of measured features \mathbf{X} so that the treatment assignment is conditionally independent of the potential outcomes.

Assumption 1. *Conditional exchangeability*

$$A \perp\!\!\!\perp Y^0, Y^1 \mid \mathbf{X}$$

This independence is referred to as conditional exchangeability (or unconfoundedness) and implies an absence of unmeasured confounding that cannot be verified with observational data (Hernán and Robins, 2020). Then there are no features, other than \mathbf{X} , that Y^0 or Y^1 depend on and that differ in distribution between individuals with $A = 1$ and $A = 0$.

Furthermore, we need to assume that the observed outcome of an individual equals the potential outcome for the treatment that is actually assigned, referred to as causal consistency.

Assumption 2. *Causal consistency*

$$Y_i^a = Y_i \mid \{A_i = a\}$$

Causal consistency is also referred to as the stable unit treatment value assumption (SUTVA)(Imbens and

Rubin, 2015). SUTVA implies that potential outcomes are independent of the treatment levels of other individuals (no interference). Causal consistency can also not be verified with data.

Finally, the probability of receiving treatment should be bounded away from 0 and 1 for all levels of \mathbf{X} , referred to as positivity (Hernán and Robins, 2020).

Assumption 3. Positivity

$$\exists \eta > 0 \forall \mathbf{x} : \eta \leq \mathbb{P}(A = 1 \mid \mathbf{X} = \mathbf{x}) \leq 1 - \eta$$

Positivity is also known as overlap (Imbens and Rubin, 2015) and can be validated with data.

As in Athey et al. (2019, Section 6), by causal consistency, we use the parameterization

$$Y_i = Y_i^0 + b_i A_i, \tag{1}$$

where b_i is the ITE of individual i , so that $Y_i^1 = Y_i^0 + b_i$. The ITE can be divided into the CATE given the features \mathbf{X}_i , $\tau(\mathbf{X}_i)$, and the individual deviation from the CATE, U_{1i} . For our purposes, it helps to reparameterize Equation (1) as

$$Y_i = \theta_0(\mathbf{X}_i) + N_{Y_i} + (\tau(\mathbf{X}_i) + U_{1i}) A_i, \tag{2}$$

where $\theta_0(\mathbf{x}) = \mathbb{E}[Y_i^0 \mid \mathbf{X}_i = \mathbf{x}]$, $\tau(\mathbf{x}) = \mathbb{E}[b_i \mid \mathbf{X}_i = \mathbf{x}]$, $\mathbb{E}[N_{Y_i} \mid \mathbf{X}_i = \mathbf{x}] = 0$ and $\mathbb{E}[U_{1i} \mid \mathbf{X}_i = \mathbf{x}] = 0$. Note that other characteristics (different from the mean) of the $N_Y \mid \mathbf{X} = \mathbf{x}$ and $U_1 \mid \mathbf{X} = \mathbf{x}$ distributions can depend on the value of \mathbf{x} . Furthermore, U_1 and N_Y can be dependent. The latter can never be studied from data without making additional assumptions due to the fundamental problem of causal inference, i.e. we cannot observe the pair (Y^0, Y^1) .

2.1 Case study and data simulation

To illustrate how the random conditional expectation $\mathbb{E}[Y^1 - Y^0 \mid \mathbf{X}]$ and $Y^1 - Y^0$ may differ in distribution, we simulate data based on the Framingham Heart Study (FHS) (Mahmood et al., 2014). We focus on the heterogeneity in the effect of non-alcoholic fatty liver disease on a clinical precursor to heart failure, the left ventricular filling pressure (Chiu et al., 2020). The association found in the original work was adjusted for age, sex, smoking, alcohol use, diabetes, systolic blood pressure (sbp), antihypertensive-med use, lipid-lowering med use, total cholesterol, high-density lipoprotein cholesterol, triglycerides and fasting glucose. However, for this illustration, we will assume that only sex and sbp are confounders. We will simulate from the following cause-effect relations

$$\begin{aligned} A_i &= \mathbb{1} \left\{ \frac{\exp(\alpha_0 + \alpha_{\text{sbp}} X_{\text{sbp},i} + \alpha_{\text{sex}} X_{\text{sex},i})}{1 - \exp(\alpha_0 + \alpha_{\text{sbp}} X_{\text{sbp},i} + \alpha_{\text{sex}} X_{\text{sex},i})} > N_{A_i} \right\} \\ Y_i^0 &= \beta_0 + \beta_{\text{sex}} X_{\text{sex},i} + \beta_{\text{sbp}} X_{\text{sbp},i} + N_{Y_i} \\ Y_i^1 &= Y_i^0 + (\tau_0 + \tau_{\text{sex}} X_{\text{sex},i} + \tau_{\text{sbp}} X_{\text{sbp},i} + U_{1i}), \end{aligned} \tag{3}$$

where $X_{\text{sex},i} \sim \text{Ber}(p)$, $X_{\text{sbp},i} \sim \mathcal{N}(0, 1)$, $U_{1i} \sim \mathcal{N}(0, \sigma_1^2)$, $N_{Y_i} \sim \mathcal{N}(0, \sigma_0^2)$, $N_{A_i} \sim \text{Uni}[0, 1]$, $U_{1i} \perp N_{Y_i}$ (and thus $U_{1i} \perp Y_i^0$). Moreover, there is no unmeasured confounding, i.e. $N_{A_i} \perp N_{Y_i}, U_{1i}$ so that $A_i \perp (Y_i^1, Y_i^0) \mid X_{\text{sex},i}, X_{\text{sbp},i}$. By causal consistency, the observed outcome $Y_i = Y_i^A$ equal Y_i^1 when $A_i = 1$ and Y_i^0 when $A_i = 0$. The parameter values are obtained by fitting a linear mixed model for the relation of fatty liver disease and the left ventricular filling pressure adjusted for standardized sbp and sex,

$$Y = \beta_0 + \beta_{\text{sex}} X_{\text{sex},i} + \beta_{\text{sbp}} X_{\text{sbp},i} + N_{Y_i} + (\tau_0 + \tau_{\text{sex}} X_{\text{sex},i} + \tau_{\text{sbp}} X_{\text{sbp},i} + U_{1i}) A_i, \tag{4}$$

to the subset of the FHS participants ($n = 2356$) as used by Chiu et al. (2020). The values obtained with PROC LOGISTIC and PROC MIXED in SAS equal $\alpha_0 = -1.7$, $\alpha_{\text{sex}} = -0.1$, $\alpha_{\text{sbp}} = 0.4$ (so that $\mathbb{P}(A = 1 \mid X_{\text{sex}} = 1) = 0.15$ and $\mathbb{P}(A = 1 \mid X_{\text{sex}} = 0) = 0.16$), $\beta_0 = 5.9$, $\beta_{\text{sex}} = 0.8$, $\beta_{\text{sbp}} = 0.5$, $\tau_0 = 0.45$,

$\tau_{\text{sex}} = 0.1$, $\tau_{\text{sbp}} = 0.15$, $\sigma_0^2 = 1.6^2$ and $\sigma_1^2 = 1.4^2$. The distribution of $Y^1 - Y^0$ is shown in Figure 1a, where $\mathbb{E}[Y^1 - Y^0] = 0.5$, $\sqrt{\text{var}(Y^1 - Y^0)} = 1.41$ and $\mathbb{P}(Y^1 - Y^0 > 0) = 0.64$. Furthermore, the distribution of the conditional expectation $\mathbb{E}[Y^1 - Y^0 \mid X_{\text{sbp}}, X_{\text{sex}}]$ is shown in Figure 1a with a standard deviation equal to 0.16 and $\mathbb{P}(\mathbb{E}[Y^1 - Y^0 \mid X_{\text{sbp}}, X_{\text{sex}}] > 0) = 1.00$. The conditional expectation distribution seriously differs from that of the ITE due to the unmeasured (remaining) effect heterogeneity (U_1). For completeness, the distributions of Y^1 and Y^0 are presented in Figure 1b. Moreover, we simulate X_0 which is a measured variable associated with the level of the individual modifier U_1 , $(U_1, X_0)^T \sim \mathcal{N}\left(\mathbf{0}, \begin{pmatrix} \sigma_1^2 & \rho\delta\sigma_1^2 \\ \rho\delta\sigma_1^2 & \delta^2\sigma_1^2 \end{pmatrix}\right)$. For $\rho > 0$, X_0 is another measured modifier. Varying ρ can thus be used to investigate cases where more of the latent individual effect modification can be explained while preserving the distribution of $Y^1 - Y^0$. All programming codes used for this work can be found online at <https://github.com/RAJP93/CATE>.

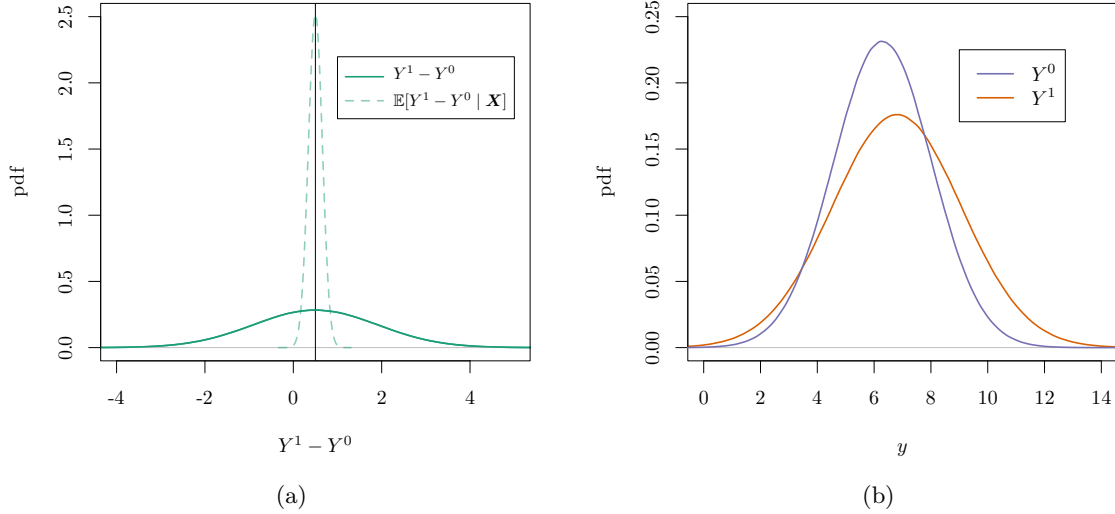


Figure 1: The ICE (a, solid line) and potential outcome (b) distributions for the cause-effect relations underlying the simulation. The ACE is presented with a vertical solid black line (a). The distribution of a random CATE, thus for random X_{sbp} and X_{sex} is also presented (a, dotted line).

2.2 Causal random forest

Using ML methods to study causal-effect heterogeneity is challenging as standard cross-validation approaches cannot be used since the actual causal effect is not observed for any individual (Athey and Imbens, 2016). Causal trees (Athey and Imbens, 2016) and causal forests (Wager and Athey, 2018) have been introduced to draw valid inferences in case of complex causal-effect heterogeneity. These papers mainly focus on data from randomized experiments and suggest adding traditional propensity score methods (Athey and Imbens, 2016) or using a different algorithm that is less sensitive to the complexity of the treatment effect function (Wager and Athey, 2018) for observational studies (without unmeasured confounding). The CRF procedure as implemented in the `causal_forest` function from the R-package `grf` is an example of a generalized random forest (GRF) (Athey et al., 2019). This CRF can be used on data from randomized experiments and observational studies without unmeasured confounding. This ML method is a random forest-based variant of the R-learner (Nie and Wager, 2020). As mentioned in the introduction, R-learners focus on the relation between normalized outcome and treatment assignment as originally used by Robinson (1988)

$$Y_i \mid \{\mathbf{X}_i = \mathbf{x}\} - \mathbb{E}[Y_i \mid \mathbf{X}_i = \mathbf{x}] = (A_i - \mathbb{E}[A_i \mid \mathbf{X}_i = \mathbf{x}]) \tilde{\tau}(\mathbf{x}) + \tilde{N}_{Y_i}, \quad (5)$$

where $\mathbb{E}[\tilde{N}_{Y_i} \mid A_i = 1, \mathbf{X}_i = \mathbf{x}] = \mathbb{E}[\tilde{N}_{Y_i} \mid A_i = 0, \mathbf{X}_i = \mathbf{x}] = 0$. Note that $\tilde{\tau}(\mathbf{x})$ represents the conditional association measure of A and Y given $\mathbf{X} = \mathbf{x}$. This association will equal the CATE for $\mathbf{X} = \mathbf{x}$ under

certain assumptions as we will show next. Using parameterization (2) we can derive

$$\begin{aligned}
Y_i | \{\mathbf{X}_i = \mathbf{x}\} - \mathbb{E}[Y_i | \mathbf{X}_i = \mathbf{x}] & \quad (6) \\
&= (\theta_0(\mathbf{x}) + N_{Y_i} + (\tau(\mathbf{x}) + U_{1i}) A_i) - (\theta_0(\mathbf{x}) + \mathbb{E}[(\tau(\mathbf{x}) + U_{1i}) A_i | \mathbf{X}_i = \mathbf{x}]) \\
&= (A_i - \mathbb{E}[A_i | \mathbf{X}_i = \mathbf{x}]) \tau(\mathbf{x}) + (A_i U_{1i} - \mathbb{E}[A_i U_{1i} | \mathbf{X}_i = \mathbf{x}] + N_{Y_i}).
\end{aligned}$$

If $\mathbb{E}[U_1 + N_Y | A = 1, \mathbf{X} = \mathbf{x}] \neq \mathbb{E}[N_Y | A = 0, \mathbf{X} = \mathbf{x}]$, then $\tilde{\tau}(\mathbf{x}) \neq \tau(\mathbf{x})$. This can occur when there is remaining (unmeasured) confounding after adjusting for \mathbf{X} . However, in absence of unmeasured confounding, i.e. $A \perp\!\!\!\perp N_Y, U_1$,

$$Y_i | \{\mathbf{X}_i = \mathbf{x}\} - \mathbb{E}[Y_i | \mathbf{X}_i = \mathbf{x}] = (A_i - \mathbb{E}[A_i | \mathbf{X}_i = \mathbf{x}]) \tau(\mathbf{x}) + (A_i U_{1i} + N_{Y_i}), \quad (7)$$

where $\mathbb{E}[U_{1i} + N_{Y_i} | A_i = 1, \mathbf{X}_i = \mathbf{x}] = \mathbb{E}[N_{Y_i} | A_i = 0, \mathbf{X}_i = \mathbf{x}] = 0$. Then, $\tilde{\tau}(\mathbf{x})$ equals $\tau(\mathbf{x})$, and thus equals the CATE for $\mathbf{X} = \mathbf{x}$.

In the absence of unmeasured confounding, the R-learner thus allows us to estimate (or predict) the CATEs, $\tau(\mathbf{x})$, from observational data. The CRF implementation of the causal random forest starts by predicting $\mathbb{E}[Y_i | \mathbf{X}_i = \mathbf{x}_i]$ and $\mathbb{E}[A_i | \mathbf{X}_i = \mathbf{x}_i]$ for each i by fitting two separate regression forests (Athey and Wager, 2019). Their out-of-bag predictions $\hat{m}^{-i}(\mathbf{x}_i)$ and $\hat{e}^{-i}(\mathbf{x}_i)$ are then used to create the centered outcomes $\tilde{Y}_i = Y_i - \hat{m}^{-i}(\mathbf{x}_i)$ and $\tilde{A}_i = A_i - \hat{e}^{-i}(\mathbf{x}_i)$ for individual i . The predictions $\hat{m}^{-i}(\mathbf{x}_i)$ and $\hat{e}^{-i}(\mathbf{x}_i)$ are only based on trees that did not use observation i during training. Subsequently, for a new set of features \mathbf{x} , similarity weights $\alpha_j(\mathbf{x})$ are produced for each observation in the sample, and $\tilde{\tau}(\mathbf{x})$ (that can be a complex function of \mathbf{x}) is estimated as

$$\hat{\tilde{\tau}}(\mathbf{x}) = \frac{\sum_{i=1}^n \alpha_i(\mathbf{x}) (Y_i - \hat{m}^{-i}(\mathbf{x}_i)) (A_i - \hat{e}^{-i}(\mathbf{x}_i))}{\sum_{i=1}^n \alpha_i(\mathbf{x}) (A_i - \hat{e}^{-i}(\mathbf{x}_i))}, \quad (8)$$

see Athey and Wager (2019) for more details. The $\alpha_j(\mathbf{x})$ are obtained by first growing a set of B (user-specified) trees. For each tree, a random subsample \mathcal{I} of the available data is taken (fraction is user-specified). The subsample is randomly divided into (by default) equally sized \mathcal{J}_1 and \mathcal{J}_2 . The honest decision tree, in the sense of Wager and Athey (2018), is only fitted on \mathcal{J}_1 and optimizes the heterogeneity in the effect of \tilde{A} on \tilde{Y} between the different nodes using gradient-based approximations of treatment-effect estimates in candidate children nodes, see Athey et al. (2019, Section 2.3). The similarity weights are first estimated per tree b , α_{bj} , and are non-zero (and equal) for those elements of \mathcal{J}_2 that fall in the same leaf as \mathbf{x} , and are averaged over all trees to obtain α_j . For individuals from the original dataset, out-of-bag predictions are made by averaging the similarity weights only over trees that did not use this particular observation during training.

The ATE is estimated using the augmented inverse probability weighting (AIPW) estimator (Robins and Rotnitzky, 1995) and equals

$$\frac{1}{n} \sum_{i=1}^n \left(\hat{\tilde{\tau}}(\mathbf{x}_i) + A_i \frac{Y_i - \hat{\mu}_{1i}(\mathbf{x}_i)}{\hat{e}^{-i}(\mathbf{x}_i)} - (1 - A_i) \frac{Y_i - \hat{\mu}_{0i}(\mathbf{x}_i)}{1 - \hat{e}^{-i}(\mathbf{x}_i)} \right), \quad (9)$$

where $\hat{\mu}_{1i}(\mathbf{x}_i) = \hat{m}^{-i}(\mathbf{x}_i) + (1 - \hat{e}^{-i}(\mathbf{x}_i)) \hat{\tilde{\tau}}(\mathbf{x}_i)$ and $\hat{\mu}_{0i}(\mathbf{x}_i) = \hat{m}^{-i}(\mathbf{x}_i) - \hat{e}^{-i}(\mathbf{x}_i) \hat{\tilde{\tau}}(\mathbf{x}_i)$. The AIPW estimator is double robust, i.e. consistent if $\hat{\tilde{\tau}}(\mathbf{x})$ or $\hat{e}(\mathbf{x})$ is a consistent estimator of $\tau(\mathbf{x})$ or $\mathbb{E}[A | \mathbf{X} = \mathbf{x}]$ respectively.

In this work, we fit a CRF to the simulated data as described in Section 2.1 to estimate the $(X_{\text{sex}}, X_{\text{sbp}}, X_0)$ -CATE for each individual. We vary the sample size, $n \in \{200, 2000, 20000\}$ and the correlation between the unmeasured modifier U_1 and the measured X_0 , $\rho \in \{0, 0.25, 0.5, 0.75, 1\}$, while fixing $\delta = 2$. We use the default settings of the `causal_forest` function, except for the $n = 200$ settings where we set `min.node.size=1`. For each simulation, we compute the empirical standard deviation (SD) and positive effect probability (PEP), $\mathbb{P}(Y^1 - Y^0 > 0)$, of the estimated CATE distribution to estimate the SD and PEP of the ITE distribution, respectively. As presented in Section 2.1, their actual values equal 0.5, 1.41, and 0.64, respectively. The ATE

is estimated with the AIPW estimator using the `average_treatment_effect` function of the `grf` package. Furthermore, based on 1000 bootstrap samples, we estimate 95% confidence intervals (CIs) for all three characteristics. Based on 1000 simulations, we estimate the bias, mean squared error (MSE) and coverage for the different settings. Finally, we estimate the ITE distribution per simulation with a Gaussian kernel density estimator over the estimated CATEs using the `density` function in R with the default settings.

3 Results

The bias, MSE and coverage for the ATE, SD and PEP of the ITE distribution based on the CATE distribution, estimated with the causal forest, are presented in Table 1 for the different settings.

Table 1: Bias, mean squared error (MSE) and coverage of the estimated mean, SD and PEP ($\mathbb{P}(Y^1 - Y^0 > 0)$) of the ITE distribution using the characteristics of the estimated CATE distribution as an estimator, based on 1000 simulated samples per setting.

ρ	n	Bias			MSE			Coverage		
		ATE	SD	PEP	ATE	SD	PEP	ATE	SD	PEP
0	200	0.05	-0.97	0.18	0.20	0.97	0.08	0.95	0.02	0.83
0	2000	-0.00	-1.18	0.33	0.02	1.39	0.11	0.94	0.00	0.20
0	20000	0.00	-1.18	0.35	0.00	1.40	0.12	0.95	0.00	0.00
0.25	200	0.01	-0.94	0.16	0.20	0.91	0.07	0.94	0.03	0.86
0.25	2000	0.00	-1.07	0.28	0.02	1.15	0.08	0.94	0.00	0.29
0.25	20000	-0.00	-1.02	0.26	0.00	1.04	0.07	0.95	0.00	0.00
0.50	200	0.02	-0.87	0.14	0.19	0.80	0.06	0.95	0.07	0.86
0.50	2000	0.01	-0.82	0.15	0.02	0.69	0.03	0.95	0.00	0.56
0.50	20000	0.00	-0.71	0.12	0.00	0.51	0.02	0.94	0.00	0.01
0.75	200	0.04	-0.73	0.12	0.16	0.58	0.04	0.95	0.19	0.87
0.75	2000	0.01	-0.53	0.06	0.01	0.29	0.01	0.95	0.00	0.85
0.75	20000	0.00	-0.38	0.05	0.00	0.15	0.00	0.94	0.00	0.51
1.00	200	0.04	-0.56	0.09	0.14	0.37	0.03	0.95	0.37	0.88
1.00	2000	0.01	-0.20	0.01	0.01	0.05	0.00	0.96	0.42	0.93
1.00	20000	0.00	-0.04	0.00	0.00	0.00	0.00	0.95	0.76	0.94

In the absence of features (X_0) that are associated with the unmeasured modifier U_1 , i.e. when $\rho = 0$, the variability in the ITE is seriously underestimated when using the CATE distribution as a proxy as shown in the first row of Figure 2. Therefore, the SD and PEP of the estimated distribution of the conditional expectation ($\mathbb{E}[Y^1 - Y^0 | \mathbf{X}]$) are biased estimators of the characteristics of the ITE distribution. The bias is the lowest for a small sample size due to the finite-sample bias, and the coverage of the PEP is not much off. For larger sample sizes, the CATE distribution can be estimated more precisely. The bias increases and the coverage decreases.

For $\rho = 0.25$, we observe the same trend. However, for $\rho \geq 0.50$, the bias is more extensive for small sample sizes. In the latter cases, the finite size bias of the CATE distribution estimator no longer compensates for the difference between the ITE and CATE distribution. Nevertheless, the uncertainty in the estimate for small sample sizes still results in higher coverage of the PEP. For $\rho = 0.75$, the CATE distribution becomes a reasonable proxy for the ITE distribution, as seen from the fourth row in Figure 2. Finally, for $\rho = 1$, U_1 equals X_0 , and there is thus no unmeasured effect modification. In this case, the flexible machine learning estimation of the CATE distribution can be used to estimate the ITE distribution and understand the variability in the treatment effect. Indeed, the bias of the SD and the PEP become small, and the coverage approaches the nominal probability. The bias of the SD is still not neglectable, so the coverage of the SD deviates from the nominal probability.

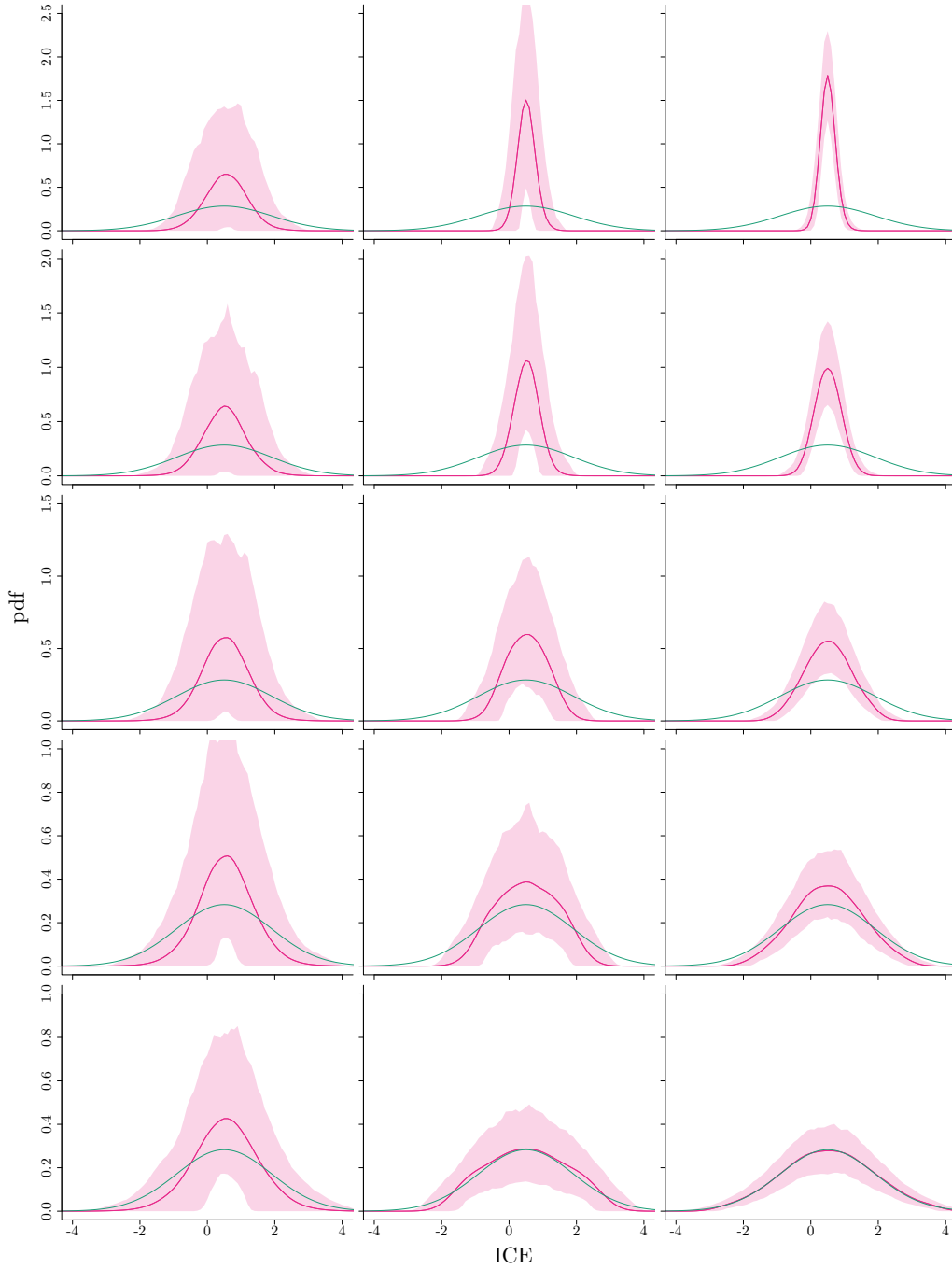


Figure 2: Pointwise empirical mean (opaque pink) as well as the 2.5% and 97.5% quantiles (transparent pink) of the estimated ITE densities of 1000 simulations. Sample size per simulation varies over the columns and equals 200 (left), 2000 (middle) and 20000 (right). The association of the measured X_0 and unmeasured modifier U_1 varies per row equal to 0, 0.25, 0.50, 0.75, 1 (top to bottom). Furthermore, the true ITE distribution is presented (green).

4 From conditional means to conditional distributions

We presented examples in which the distribution of $\mathbb{E}[Y^1 - Y^0 \mid \mathbf{X}]$ differ from that of $Y^1 - Y^0$. To overcome this issue, we should consider the remaining effect heterogeneity. In this section, we show that the variance of $Y^1 - Y^0 \mid \mathbf{X} = \mathbf{x}$ is only identifiable when we are willing to make another causal assumption that cannot

be verified on data (as is the case for Assumption 1). Under this assumption, we can extend the CRF algorithm by also estimating the conditional variance of the effect for each individual. From Equation (2), we can derive that the variance of $Y^1 - Y^0 \mid \mathbf{X} = \mathbf{x}$ equals

$$\mathbb{E}[(\tau(\mathbf{x}) + U_1)^2 \mid \mathbf{X} = \mathbf{x}] - \mathbb{E}[\tau(\mathbf{x}) + U_1 \mid \mathbf{X} = \mathbf{x}]^2 = \mathbb{E}[U_1^2 \mid \mathbf{X} = \mathbf{x}]. \quad (10)$$

The conditional variance of the ITE affects the squared observed outcomes as

$$\begin{aligned} (Y_i)^2 \mid \{\mathbf{X}_i = \mathbf{x}\} &= (\theta_0(\mathbf{x}))^2 + \mathbb{E}[N_{Y_i}^2 \mid \mathbf{X}_i = \mathbf{x}] + \\ &(\tau(\mathbf{x})^2 + \mathbb{E}[U_{1_i}^2 \mid \mathbf{X}_i = \mathbf{x}] + \tau(\mathbf{x})\theta_0(\mathbf{x}) + \mathbb{E}[N_{Y_i}U_{1_i} \mid \mathbf{X}_i = \mathbf{x}]) A_i + \gamma_i^*, \end{aligned} \quad (11)$$

where $\gamma_i^* = N_{Y_i}^* + 2\theta_0(\mathbf{x})N_{Y_i} + (U_{1_i}^* + 2\tau(\mathbf{x})U_{1_i} + \tau(\mathbf{x})N_{Y_i} + \theta_0(\mathbf{x})U_{1_i} + \gamma_i) A_i$, $\gamma_i = N_{Y_i}U_{1_i} - \mathbb{E}[N_{Y_i}U_{1_i} \mid \mathbf{X}_i = \mathbf{x}]$, $N_{Y_i}^* = (N_{Y_i})^2 - \mathbb{E}[(N_{Y_i})^2 \mid \mathbf{X}_i = \mathbf{x}]$, $U_{1_i}^* = (U_{1_i})^2 - \mathbb{E}[(U_{1_i})^2 \mid \mathbf{X}_i = \mathbf{x}]$ so that $\mathbb{E}[N_{Y_i}^* \mid \mathbf{X}_i = \mathbf{x}] = 0$, $\mathbb{E}[U_{1_i}^* \mid \mathbf{X}_i = \mathbf{x}] = 0$, $\mathbb{E}[\gamma_i \mid \mathbf{X}_i = \mathbf{x}] = 0$ and $\mathbb{E}[\gamma_i^* \mid \mathbf{X}_i = \mathbf{x}] = 0$. In the absence of unmeasured confounding, the Robinson decomposition now reads

$$\begin{aligned} (Y_i)^2 \mid \{\mathbf{X}_i = \mathbf{x}\} - \mathbb{E}[(Y_i)^2 \mid \mathbf{X}_i = \mathbf{x}] &= \\ (A_i - \mathbb{E}[A_i \mid \mathbf{X}_i = \mathbf{x}]) (\tau(\mathbf{x})^2 + \mathbb{E}[U_{1_i}^2 \mid \mathbf{X}_i = \mathbf{x}] + \tau(\mathbf{x})\theta_0(\mathbf{x}) + \mathbb{E}[N_{Y_i}U_{1_i} \mid \mathbf{x}]) + \gamma_i^*. \end{aligned} \quad (12)$$

The decomposition thus enables us to estimate $\tau(\mathbf{x})^2 + \mathbb{E}[U_1^2 \mid \mathbf{X} = \mathbf{x}] + \tau(\mathbf{x})\theta_0(\mathbf{x}) + \mathbb{E}[N_Y U_1 \mid \mathbf{X} = \mathbf{x}]$ from observational data. Subsequently, we can estimate $\mathbb{E}[U_1^2 \mid \mathbf{X} = \mathbf{x}] + \mathbb{E}[N_Y U_1 \mid \mathbf{X} = \mathbf{x}]$ by subtracting an estimate of $\tau(\mathbf{x})^2 + \tau(\mathbf{x})\theta_0(\mathbf{x})$. However, as a result of the fundamental problem of causal inference we can never learn the joint distribution of $(N_Y, U_1) \mid \mathbf{X} = \mathbf{x}$, and neither $\mathbb{E}[N_Y U_1 \mid \mathbf{X} = \mathbf{x}]$. Thus, we cannot estimate the variance of $Y^1 - Y^0 \mid \mathbf{X} = \mathbf{x}$, $\mathbb{E}[U_1^2 \mid \mathbf{X} = \mathbf{x}]$, without an additional assumption. If we can assume that $U_1 \perp\!\!\!\perp N_Y \mid \mathbf{X} = \mathbf{x}$, or equivalently $U_1 \perp\!\!\!\perp Y^0 \mid \mathbf{X} = \mathbf{x}$, then the variance of the causal effect given \mathbf{X} can be estimated since the independence implies that $\mathbb{E}[N_Y U_1 \mid \mathbf{X} = \mathbf{x}] = 0$. The assumption implies conditional independence of the outcome under no treatment and the effect, i.e. the deviation of $Y^0 \mid \mathbf{X} = \mathbf{x}$ from $\mathbb{E}[Y^0 \mid \mathbf{X} = \mathbf{x}]$ is independent of the deviation of $Y^1 - Y^0 \mid \mathbf{X} = \mathbf{x}$ from the CATE. Therefore, we refer to this assumption as conditional independent effect deviation.

Assumption 4. Conditional independent effect deviation

$$Y^1 - Y^0 \perp\!\!\!\perp Y^0 \mid \mathbf{X} = \mathbf{x}$$

If Assumption 4 (in addition to 1, 2 and 3) holds, then $\text{var}(Y^1 - Y^0 \mid \mathbf{X} = \mathbf{x})$ can be estimated as (15) with the extended CRF. Moreover, note that if the ITE equals the CATE, then $\forall i : U_{1_i} = 0$ so that $\mathbb{E}[U_1^2 \mid \mathbf{X} = \mathbf{x}] + \mathbb{E}[N_Y U_1 \mid \mathbf{X} = \mathbf{x}] = 0$ anyway.

To estimate $\tau(\mathbf{x})^2 + \mathbb{E}[U_1^2 \mid \mathbf{X} = \mathbf{x}] + \tau(\mathbf{x})\theta_0(\mathbf{x}) + \mathbb{E}[N_Y U_1 \mid \mathbf{X} = \mathbf{x}]$, we first fit a separate regression forest to estimate $\mathbb{E}[(Y_i)^2 \mid \mathbf{X}_i = \mathbf{x}_i]$, and use it's out-of-bag predictions $\hat{m}^{-i}(\mathbf{x}_i)$ to create the centered outcome $\widetilde{Y}_i^2 = Y_i^2 - \hat{m}^{-i}(\mathbf{x}_i)$ for individual i . We use again the similarity weights obtained from the original CRF for neighbouring matching and estimate $\tau(\mathbf{x})^2 + \mathbb{E}[U_1^2 \mid \mathbf{X} = \mathbf{x}] + \tau(\mathbf{x})\theta_0(\mathbf{x}) + \mathbb{E}[N_Y U_1 \mid \mathbf{X} = \mathbf{x}]$ as

$$\frac{\sum_{i=1}^n \alpha_i(\mathbf{x}) \left(Y_i^2 - \hat{m}^{-i}(\mathbf{x}_i) \right) (A_i - \hat{e}^{-i}(\mathbf{x}_i))}{\sum_{i=1}^n \alpha_i(\mathbf{x}) (A_i - \hat{e}^{-i}(\mathbf{x}_i))}. \quad (13)$$

As in the original CRF, for \mathbf{x} contained in the observed data, out-of-bag predictions are made by averaging the similarity weights over trees that did not use this particular observation during training. Subsequently, we estimate $\mathbb{E}[U_1^2 \mid \mathbf{X} = \mathbf{x}] + \mathbb{E}[N_Y U_1 \mid \mathbf{X} = \mathbf{x}]$, by subtracting the estimate of $\tau(\mathbf{x})^2 + \tau(\mathbf{x})\theta_0(\mathbf{x})$ obtained from the original CRF algorithm equal to

$$\hat{\tau}(\mathbf{x}_i)^2 + \hat{\tau}(\mathbf{x}_i)\hat{\mu}_{0_i}(\mathbf{x}_i), \quad (14)$$

where $\hat{\mu}_{0_i}(\mathbf{x}_i) = \hat{m}^{-i}(\mathbf{x}_i) - \hat{e}^{-i}(\mathbf{x}_i)\hat{\tau}(\mathbf{x}_i)$ as also used in (9).

Under Assumption 4 (as well as 1, 2 and 3), the extended CRF algorithm can be used to estimate the conditional ITE variance, $\mathbb{E}[U_1^2 \mid \mathbf{X} = \mathbf{x}]$, as

$$\frac{\sum_{i=1}^n \alpha_i(\mathbf{x}) \left(Y_i^2 - \hat{m}^{-i}(\mathbf{x}_i) \right) (A_i - \hat{e}^{-i}(\mathbf{x}_i))}{\sum_{i=1}^n \alpha_i(\mathbf{x}) (A_i - \hat{e}^{-i}(\mathbf{x}_i))} - \hat{\tau}(\mathbf{x}_i)^2 - \hat{\tau}(\mathbf{x}_i) \hat{\mu}_{0i}(\mathbf{x}_i), \quad (15)$$

in addition to the CATE estimation presented in (8). To estimate the ITE distribution, we can approximate the distribution of $Y^1 - Y^0 \mid \mathbf{X} = \mathbf{x}$ with a Gaussian distribution so that in the case of no remaining effect heterogeneity the variance is zero and the distribution is degenerate in the CATE. By the law of total probability,

$$\mathbb{P}(Y^1 - Y^0 \leq y) = \int \mathbb{P}(Y^1 - Y^0 \leq y \mid \mathbf{X} = \mathbf{x}) dF_{\mathbf{X}}(\mathbf{x}). \quad (16)$$

We will use the extended CRF to estimate the ITE distribution from the simulated datasets. The ATE estimate will remain unchanged, the PEP is now estimated as $n^{-1} \sum_{i=1}^n \mathbb{P}(Z_i > 0)$, where $Z_i \sim \mathcal{N}(\hat{\tau}(\mathbf{x}_i), \hat{\mathbb{E}}[U_1^2 \mid \mathbf{X} = \mathbf{x}_i])$, and the SD as $\sqrt{n^{-1} \left(\sum_{i=1}^n \hat{\tau}(\mathbf{x}_i)^2 + \hat{\mathbb{E}}[U_1^2 \mid \mathbf{X} = \mathbf{x}_i] \right) - \widehat{\text{ATE}}^2}$.

4.1 Results resumed

The bias, MSE and coverage for the ATE, SD and PEP of the ITE distribution, respectively, using the extended causal forest and assuming Gaussian distributed $Y^1 - Y^0 \mid \mathbf{X} = \mathbf{x}$ are presented in Table 2 for the different settings of the simulation study described in Section 2.1.

Table 2: Bias, mean squared error (MSE) and coverage of the estimated ATE, SD and PEP ($\mathbb{P}(Y^1 - Y^0 > 0)$) of the ITE distribution using the characteristics of the estimated CATE as an estimator based on 1000 simulated samples per setting.

ρ	n	Bias			MSE			Coverage		
		ATE	SD	PEP	ATE	SD	PEP	ATE	SD	PEP
0	200	0.05	-0.06	0.04	0.20	0.25	0.02	0.95	0.90	0.91
0	2000	-0.00	0.04	0.01	0.02	0.02	0.00	0.94	0.93	0.90
0	20000	0.00	0.03	0.01	0.00	0.00	0.00	0.95	0.89	0.82
0.25	200	0.01	-0.08	0.03	0.20	0.29	0.02	0.94	0.88	0.92
0.25	2000	0.00	0.04	0.01	0.02	0.02	0.00	0.94	0.93	0.90
0.25	20000	-0.00	0.04	0.00	0.00	0.00	0.00	0.95	0.86	0.86
0.50	200	0.02	-0.07	0.03	0.19	0.27	0.02	0.95	0.90	0.92
0.50	2000	0.01	0.05	0.01	0.02	0.02	0.00	0.95	0.94	0.91
0.50	20000	0.00	0.05	0.00	0.00	0.00	0.00	0.94	0.80	0.92
0.75	200	0.04	-0.07	0.03	0.16	0.26	0.02	0.95	0.92	0.92
0.75	2000	0.01	0.07	-0.00	0.01	0.03	0.00	0.95	0.91	0.94
0.75	20000	0.00	0.07	-0.00	0.00	0.01	0.00	0.94	0.71	0.93
1.00	200	0.04	-0.03	0.02	0.14	0.26	0.02	0.95	0.91	0.92
1.00	2000	0.01	0.09	-0.01	0.01	0.03	0.00	0.96	0.90	0.93
1.00	20000	0.00	0.09	-0.01	0.00	0.01	0.00	0.95	0.56	0.89

In the case of remaining heterogeneity ($\rho < 1$), the bias of the SD estimator using the extended CRF is much lower than using the CRF. For larger sample sizes ($n = 2000$ and $n = 20000$), the small bias is of the opposite sign to the one using the CRF. The bias of the PEP is also seriously decreased. For all settings, the MSE of the extended estimator is smaller for both the SD and PEP. Also, the coverage of the SD and PEP did considerably improve. However, for $n = 20000$ and $\rho = 0.50$ or $\rho = 0.75$, the coverage probability of the SD did deviate from the nominal level due to the small bias and the narrow CIs.

For the $\rho = 1$ case, where all variability in causal effect could be explained with the measured features, the extended CRF performs well. Only when $n = 20000$ the bias of the SD estimator using the extended CRF is slightly higher than for the original estimator due to an overspecified model. The difference is so

small that the MSE is of the same magnitude. In this case, the coverage again deviates from the nominal level and is now slightly lower than the coverage using the traditional CRF.

The pointwise mean (and 95% CI) of the estimated probability density function of the ITE distribution from 1000 simulations is presented in Figure 3 for the different settings. The extended CRF is expected to recover the ITE distribution well for all settings.

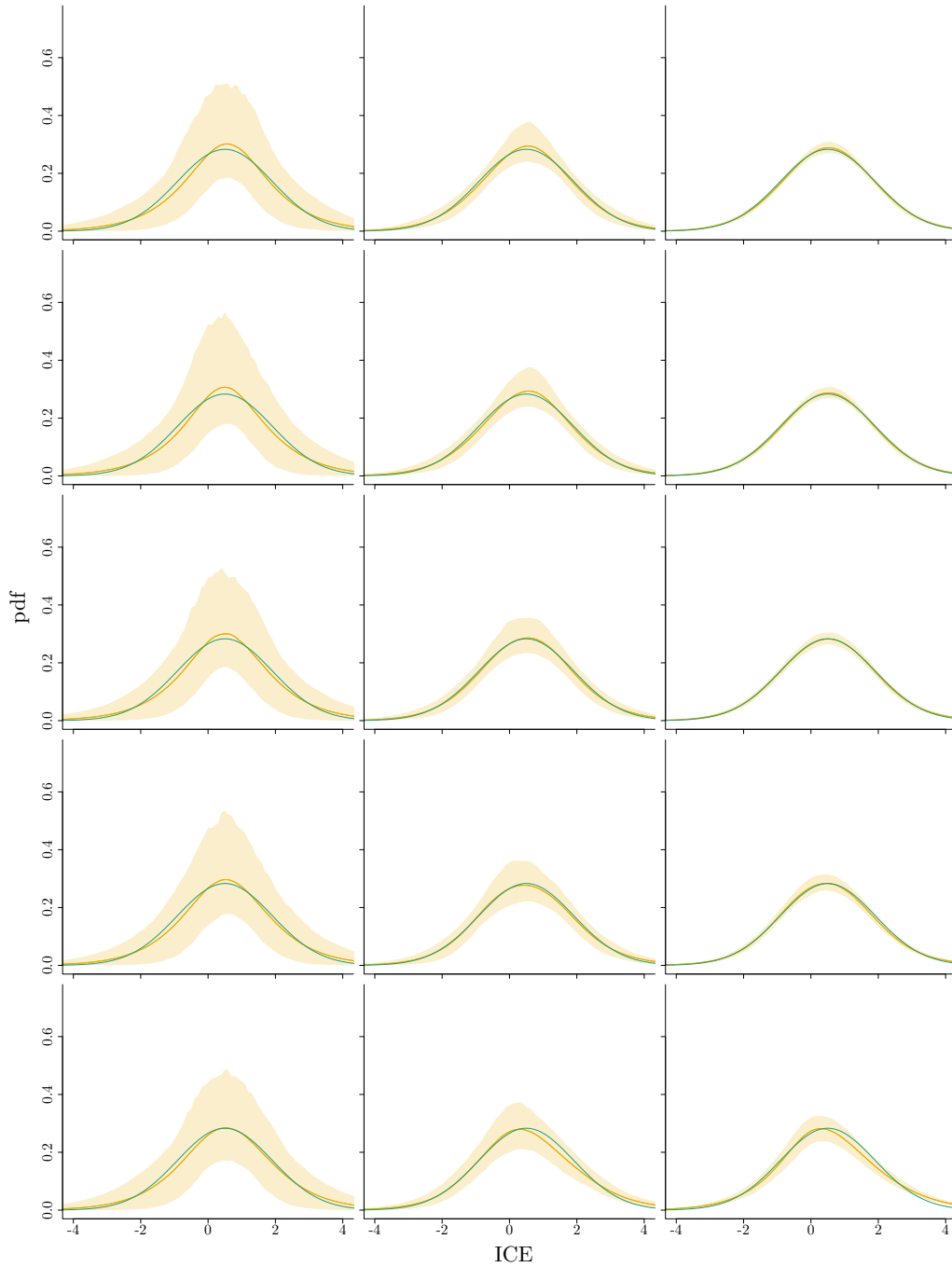


Figure 3: Pointwise empirical mean (opaque yellow) as well as the 2.5% and 97.5% quantiles (transparent yellow) of the estimated ITE densities using the extended causal forest of 1000 simulations. Sample size per simulation varies over the columns and equals 200 (left), 2000 (middle) and 20000 (right). The association of the measured X_0 and unmeasured modifier U_1 varies per row equal to 0, 0.25, 0.50, 0.75, 1 (top to bottom). Furthermore, the actual ITE distribution is presented (green).

5 Concluding remarks

Machine learning methods are of great value in understanding effect heterogeneity using CATEs. In this paper, we have shown that there might be individual effect modifications that cannot be explained by the features collected. As a result, the individualized CATE can still seriously differ from the ICE so that the ITE distribution cannot be identified by the distribution of the (random) conditional expectation alone. Applied researchers must be aware of this possible discrepancy. For example, the remaining effect heterogeneity beyond heterogeneity in the CATEs can result in a lack of generalizability since the distribution of unmeasured effect modifiers in other populations might seriously differ from that in the sample (Seamans et al., 2021).

Studying the remaining effect heterogeneity is challenging as the fundamental problem of causal inference prevents us from learning the joint distribution of potential outcomes. Nevertheless, one can check whether the conditional second moments of the treated and the controls are similar or whether there exists remaining effect heterogeneity. Comparing the moments can be done without making additional (untestable) assumptions next to conditional exchangeability, causal consistency and positivity. As an example, we have extended the CRF algorithm (Athey et al., 2019) also to estimate the difference in conditional variance between treated and controls. In case differences in variances are obtained, the ITE distribution cannot be explained by the CATEs alone. The increased variance among the treated is due to the ITE’s conditional variance and the covariance of the ITE and Y^0 . Therefore, to estimate the (conditional) variance of the ITE, we need to assume how the ITE and Y^0 are correlated. In this work, we have taken $Y^1 - Y^0 \perp\!\!\!\perp Y^0 \mid \mathbf{X} = \mathbf{x}$ so that the causal assumption of conditional independent effect deviation applies. Under this assumption, the conditional variance of the ITE can be estimated next to the expected effect for each individual. As a result, in contrast to the CRF, the extended CRF can be used to estimate the ITE distribution’s variance unbiasedly. When assuming that the conditional ITE distributions can be approximated with Gaussian distributions, as done in our example, the ITE distribution can also be accurately estimated. In the absence of remaining effect heterogeneity, the estimated individual variance will be small, indicating that the CATE can be used as an appropriate proxy for the ICE.

Similarly, other ML algorithms can be extended to estimate the conditional second (or higher) moments. However, it is important to realize that objective functions are chosen to maximize heterogeneity in CATEs, and the algorithms might thus not account for confounders that are no effect modifiers. Therefore, one should always verify that the distribution of potential outcomes is correctly linked to the observed distribution. In Appendix A, we illustrate that for the CRF, the orthogonalization step facilitates this link. Without this step, even the ATE estimate can be biased. Although the presented extended CRF algorithm can be used in practice, we want to emphasize that our main aim was to open up the field of (conditional) ITE distribution estimation under the conditional independent effect deviation assumption.

References

- Athey S, Imbens GW (2016) Recursive partitioning for heterogeneous causal effects. *Proceedings of the National Academy of Sciences* 113(27):7353–7360
- Athey S, Wager S (2019) Estimating Treatment Effects with Causal Forests: An Application. *Observational studies* 5(2):37–51
- Athey S, Tibshirani J, Wager S (2019) Generalized random forests. *Annals of Statistics* 47(2):1179–1203
- Balzer LB, Petersen ML (2021) Invited Commentary: Machine Learning in Causal Inference—How Do I Love Thee? Let Me Count the Ways. *American Journal of Epidemiology* 190(8):1483–1487
- Bica I, Alaa AM, Lambert C, van der Schaar M (2021) From real-world patient data to individualized treatment effects using machine learning: Current and future methods to address underlying challenges. *Clinical Pharmacology & Therapeutics* 109(1):87–100

- Blakely T, Lynch J, Simons K, Bentley R, Rose S (2019) Reflection on modern methods: when worlds collide—prediction, machine learning and causal inference. *International Journal of Epidemiology* 49(6):2058–2064
- Caron A, Baio G, Manolopoulou I (2022) Estimating individual treatment effects using non-parametric regression models: A review. *Journal of the Royal Statistical Society: Series A (Statistics in Society)* 185(3):1115–1149
- Chernozhukov V, Chetverikov D, Demirer M, Dufo E, Hansen C, Newey W, Robins JM (2018) Double/debiased machine learning for treatment and structural parameters. *The Econometrics Journal* 21(1):C1–C68
- Chiu LS, Pedley A, Massaro JM, Benjamin EJ, Mitchell GF, McManus DD, Aragam J, Vasan RS, Cheng S, Long MT (2020) The association of non-alcoholic fatty liver disease and cardiac structure and function—framingham heart study. *Liver International* 40(10):2445–2454
- Cui P, Athey S (2022) Stable learning establishes some common ground between causal inference and machine learning. *Nature Machine Intelligence* 4(2):110–115
- Curth A, van der Schaar M (2021) Nonparametric estimation of heterogeneous treatment effects: From theory to learning algorithms. In: Banerjee A, Fukumizu K (eds) *Proceedings of The 24th International Conference on Artificial Intelligence and Statistics*, PMLR, *Proceedings of Machine Learning Research*, vol 130, pp 1810–1818
- Dickerman BA, Hernán MA (2020) Counterfactual prediction is not only for causal inference. *European Journal of Epidemiology* 35(7):615–617
- Dickerman BA, Dahabreh IJ, Cantos KV, Logan RW, Lodi S, Rentsch CT, Justice AC, Hernán MA (2022) Predicting counterfactual risks under hypothetical treatment strategies: an application to HIV. *European Journal of Epidemiology* 37(4):367–376
- Fan Q, Hsu YC, Lieli RP, Zhang Y (2022) Estimation of conditional average treatment effects with high-dimensional data. *Journal of Business & Economic Statistics* 40(1):313–327
- Foster JC, Taylor JM, Ruberg SJ (2011) Subgroup identification from randomized clinical trial data. *Statistics in Medicine* 30(24):2867–2880
- van Geloven N, Swanson SA, Ramspek CL, Luijken K, van Diepen M, Morris TP, Groenwold RH, van Houwelingen HC, Putter H, le Cessie S (2020) Prediction meets causal inference: the role of treatment in clinical prediction models. *European Journal of Epidemiology* 35(7):619–630
- Green DP, Kern HL (2012) Modeling heterogeneous treatment effects in survey experiments with bayesian additive regression trees. *Public Opinion Quarterly* 76(3):491–511
- Hahn PR, Murray JS, Carvalho CM (2020) Bayesian regression tree models for causal inference: Regularization, confounding, and heterogeneous effects (with discussion). *Bayesian Analysis* 15(3):965–1056
- Hand DJ (1992) On comparing two treatments. *The American Statistician* 46(3):190–192
- Hernán MA, Robins JM (2020) *Causal Inference: What If*. Boca Raton: Chapman & Hall/CRC, Boca Raton, Florida
- Hernán MA, Hsu J, Healy B (2019) A second chance to get causal inference right: A classification of data science tasks. *CHANCE* 32(1):42–49
- Hill JL (2011) Bayesian nonparametric modeling for causal inference. *Journal of Computational and Graphical Statistics* 20(1):217–240

- Holland PW (1986) Statistics and causal inference. *Journal of the American Statistical Association* 81(396):945–960
- Imai K, Ratkovic M (2013) Estimating treatment effect heterogeneity in randomized program evaluation. *Annals of Applied Statistics* 7(1):443–470
- Imbens GW, Rubin DB (2015) *Causal Inference for Statistics, Social, and Biomedical Sciences: An Introduction*. Cambridge University Press
- Kennedy EH (2020) Optimal doubly robust estimation of heterogeneous causal effects
- Knaus MC, Lechner M, Strittmatter A (2020) Machine learning estimation of heterogeneous causal effects: Empirical Monte Carlo evidence. *The Econometrics Journal* 24(1):134–161
- Kosorok MR, Laber EB (2019) Precision medicine. *Annual Review of Statistics and Its Application* 6(1):263–286
- Kravitz R, Duan N, Braslow J (2004) Evidence-based medicine, heterogeneity of treatment effects, and the trouble with averages. *Milbank Quarterly* 82(4):661–687
- Künzel SR, Sekhon JS, Bickel PJ, Yu B (2019) Metalearners for estimating heterogeneous treatment effects using machine learning. *Proceedings of the National Academy of Sciences* 116(10):4156–4165
- van der Laan MJ, Rose S (2011) *Targeted Learning: Causal Inference for Observational and Experimental Data*. Springer, New York
- Lu M, Sadiq S, Feaster DJ, Ishwaran H (2018) Estimating Individual Treatment Effect in Observational Data Using Random Forest Methods. *Journal of Computational and Graphical Statistics* 27(1):209–219
- Mahmood SS, Levy D, Vasan RS, Wang TJ (2014) The framingham heart study and the epidemiology of cardiovascular disease: a historical perspective. *The Lancet* 383(9921):999–1008
- Mooney SJ, Pejaver V (2018) Big data in public health: Terminology, machine learning, and privacy. *Annual Review of Public Health* 39(1):95–112
- Mooney SJ, Keil AP, Westreich DJ (2021) Thirteen Questions About Using Machine Learning in Causal Research (You Won’t Believe the Answer to Number 10!). *American Journal of Epidemiology* 190(8):1476–1482
- Naimi AI, Mishler AE, Kennedy EH (2021) Challenges in Obtaining Valid Causal Effect Estimates with Machine Learning Algorithms. *American Journal of Epidemiology*
- Neyman J (1923) On the Application of Probability Theory to Agricultural Experiments. *Essay on Principles. Statistical Science* 5(4):465–472
- Nie X, Wager S (2020) Quasi-oracle estimation of heterogeneous treatment effects. *Biometrika* 108(2):299–319
- Powers S, Qian J, Jung K, Schuler A, Shah NH, Hastie T, Tibshirani R (2018) Some methods for heterogeneous treatment effect estimation in high dimensions. *Statistics in Medicine* 37(11):1767–1787
- Prosperi M, Guo Y, Sperrin M, Koopman JS, Min JS, He X, Rich S, Wang M, Buchan IE, Bian J (2020) Causal inference and counterfactual prediction in machine learning for actionable healthcare. *Nature Machine Intelligence* 2(7):369–375
- Robertson SE, Leith A, Schmid CH, Dahabreh IJ (2020) Assessing Heterogeneity of Treatment Effects in Observational Studies. *American Journal of Epidemiology* 190(6):1088–1100

- Robins JM, Rotnitzky A (1995) Semiparametric efficiency in multivariate regression models with missing data. *Journal of the American Statistical Association* 90(429):122–129
- Robins JM, Rotnitzky A, Zhao LP (1994) Estimation of regression coefficients when some regressors are not always observed. *Journal of the American Statistical Association* 89(427):846–866
- Robinson PM (1988) Root-n-consistent semiparametric regression. *Econometrica* 56(4):931–954
- Rubin DB (1974) Estimating causal effects of treatments in randomized and nonrandomized studies. *Journal of Educational Psychology* 66(5):688–701
- Schuler MS, Rose S (2017) Targeted Maximum Likelihood Estimation for Causal Inference in Observational Studies. *American Journal of Epidemiology* 185(1):65–73
- Seamans MJ, Hong H, Ackerman B, Schmid I, Stuart EA (2021) Generalizability of subgroup effects. *Epidemiology* 32(3):389–392
- Talisa VB, Chang CCH (2021) Learning and confirming a class of treatment responders in clinical trials. *Statistics in Medicine* 40(22):4872–4889
- Wager S, Athey S (2018) Estimation and Inference of Heterogeneous Treatment Effects using Random Forests. *Journal of the American Statistical Association* 113(523):1228–1242
- Wendling T, Jung K, Callahan A, Schuler A, Shah NH, Gallego B (2018) Comparing methods for estimation of heterogeneous treatment effects using observational data from health care databases. *Statistics in Medicine* 37(23):3309–3324

A Linking potential and observed outcomes

Machine learning methods can be used to fit complex heterogeneity in $\mathbb{E}[Y|A = 1, \mathbf{X} = \mathbf{x}] - \mathbb{E}[Y|A = 0, \mathbf{X} = \mathbf{x}]$. However, to estimate CATEs appropriately, $\mathbb{E}[Y|A = a, \mathbf{X} = \mathbf{x}]$ should equal $\mathbb{E}[Y^a | \mathbf{X} = \mathbf{x}]$. Thus, we should accurately account for confounding. When using the CRF to estimate CATEs, the R-learner decomposition facilitates this, as described in Section 2.2. In case this decomposition is not used, and the CATE is estimated as

$$\hat{\tau}(\mathbf{x}) = \frac{\sum_{i=1}^n \alpha_i(\mathbf{x}) Y_i A_i}{\sum_{i=1}^n \alpha_i(\mathbf{x}) A_i} - \frac{\sum_{i=1}^n \alpha_i(\mathbf{x}) Y_i (1 - A_i)}{\sum_{i=1}^n \alpha_i(\mathbf{x}) (1 - A_i)}, \quad (17)$$

where now also the similarity weights $\alpha_i(\mathbf{x})$ are obtained from a random forest fitted on the non-centralized outcome and treatment, confounders that are no effect modifiers will not be accounted for. This estimator is implemented in the `grf` package by using `causal_forest(X, Y, W, Y.hat=0, W.hat=0)`.

Consider for example the system as described in Section 2.1 modified with $\tau_{\text{sex}} = 0$ such that sex is a confounder but not a modifier. In Figure 4a, we present $\mathbb{E}[Y^1 - Y^0 | \mathbf{X}_i] - \hat{\tau}(\mathbf{X}_i)$ for the GRF with (CRF, pink) and without (yellow) using the R-learner decomposition fitted on 1000 simulations with $n = 10000$. As just explained, the R-learner decomposition is necessary to account for the confounding by sex. Otherwise, the CATE estimates (as well as the ATE estimate) are biased.

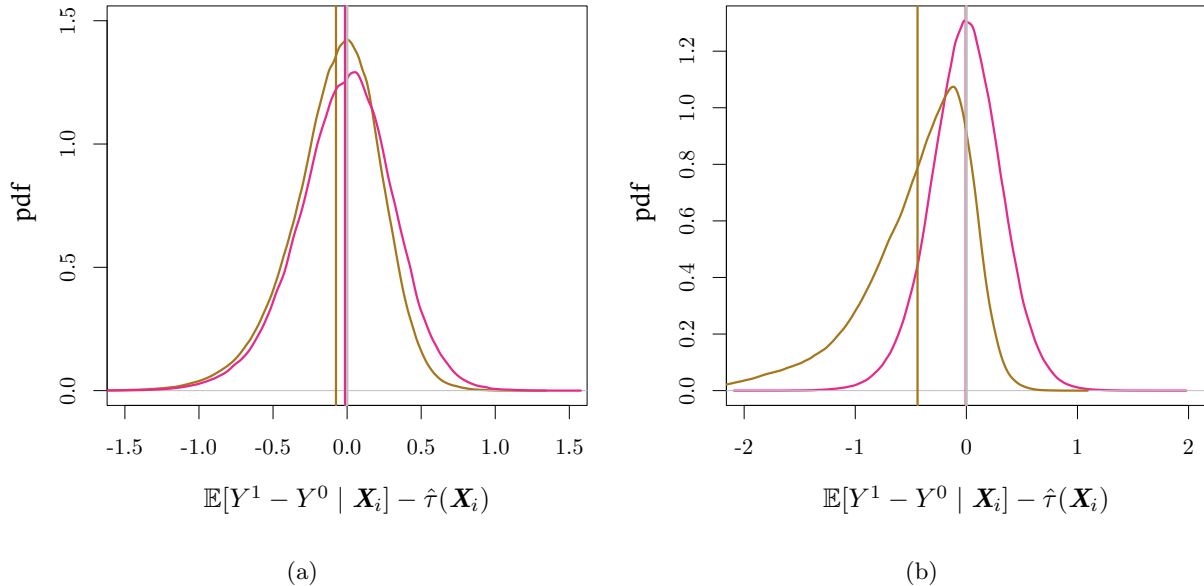


Figure 4: Density of $\mathbb{E}[Y^1 - Y^0 | \mathbf{X}_i] - \hat{\tau}(\mathbf{X}_i)$ with $\hat{\tau}(\mathbf{x})$ obtained with the default CRF (pink) and the GRF without the R-learner decomposition (yellow) based on 1000 simulations with each $n = 10000$ individuals. Furthermore, the means are presented with vertical lines. The bias resulting from the lack of confounder adjustment becomes particularly clear from the setting with extreme confounding (b).

To stress the importance of the R-learner decomposition we change the strength of the confounding relation by increasing α_{sex} to 3 and β_{sex} to 3.2 such that $\mathbb{P}(A = 1 | X_{\text{sex}} = 1) = 0.78$ and $\mathbb{P}(A = 1 | X_{\text{sex}} = 0) = 0.16$. For this more extreme setting the density of $\mathbb{E}[Y^1 - Y^0 | \mathbf{X}_i] - \hat{\tau}(\mathbf{X}_i)$ is presented in Figure 4b, and the bias becomes more apparent.

When interested in the heterogeneity of effects, the objective function of a ML method is typically focused on maximizing the heterogeneity in differences between observed treated and controls as a function of the features (\mathbf{X}) at hand. As a result, confounders that are no effect modifiers might not be accounted for by the method, and biased causal effects are obtained.